Fabrication of Electrically Controllable Microlens Array Using Liquid Crystals

Jae-Hoon Kim and Satyendra Kumar

***Abstract*—Electrically controllable liquid-crystal (LC) microlens arrays have been fabricated using the process of anisotropic phase separation of the LC from its solution in a ultraviolet curable prepolymer. The focal length of nematic LC-based microlens arrays can be changed in milliseconds with an applied electric field. The ferroelectric LC microlens array exhibits the memory effect and modulates the transmitted light within a few microseconds, i.e., $\sim$ 1000 times faster than the nematic LC-based microlens. Having no internal substructures to scatter light, these devices offer high efficiency and high light throughput that is different from polymer-dispersed devices.**

***Index Terms*—Anisotropic phase separation, liquid crystal (LC), memory effect, microlens array.**

I. Introduction

With the advancements in computing and communications technology, there is a growing and critical need for real-time reconfigurable optical elements such as fast optical switches, beam-steering (e.g., diffractive gratings), and wave front-shaping (e.g., microlens array) devices for use in high-density data storage, optical interconnects, beam modulating, and energy-directing devices. The ability to electrically control the action of these devices is a key requirement. A number of attempts have been made to construct liquid-crystal (LC)-based real-time reconfigurable microlens arrays to perform real-time optical interconnection in optical computing and photonic switching circuits [1], [2]. The technology required to realize such *active* microlenses is fundamentally different from that used in *passive* devices built using surface relief structures [3]–[5]. Methods employed in the previous studies to build electrically controllable microlens arrays include 1) a combination of a passive solid-state lens array and an LC modulator [6] and 2) a gradient refractive-index (GRIN) profile of LC produced with an axially symmetric electric field generated by specially designed electrode patterns for each microlens [1], [2].

On the other hand, a method of preparing LC devices using one-dimensional anisotropic phase separation of a LC from its solution in a polymer that results in adjacent layers of LC and polymer has been developed recently. These systems are known as phase-separated composite organic films (PSCOFs) [7] and have unique structures and electrooptical properties not observed in devices prepared by conventional methods or by other phase separation techniques, such as polymer dispersion and polymer stabilization. Since the PSCOF technology has advantages in the ease of fabrication, mechanical ruggedness, and flexibility of fine-tuning the optical path length, it is suitable for the devices in optical communication. This paper reports a simple method to fabricate an LC-based switchable microlens array using the three-dimensional (3-D) anisotropic phase separation technique, which is a modification of the PSCOF method. The focal length of the nematic LC-based microlens array can be changed in milliseconds with an applied electric field. The ferroelectric LC (FLC) microlens array exhibits the memory effect and modulates the transmitted light within a few microseconds, i.e., $\sim$ 1000 times faster than the nematic LC-based microlens.

TABLE I
Summary of the Ordinary and Extraordinary Refractive Indexes of the Materials at 590 nm

Materials	Ordinary (n_o)	Extraordinary(n_e)
E-31	1.533	1.792
Felix 15-100	1.490	1.664
NOA 65	n_p=1.524	

II. Experimental

The materials used in this study are commercial nematic E-31 (Merck Chemical Company), ferroelectric Felix 15–100 (Clariant), and photocurable prepolymer NOA-65 (Norland). In Table I, we summarize the ordinary and extraordinary refractive indexes for the materials.

Cell spacing is controlled with the use of glass fiber or bead spacers of 3–25-μm diameter. To align the LC, cells are made using substrates coated with rubbed films of poly–vinyl–alcohol (PVA) or Nylon 6 (N6). We note that the results of phase separation are greatly affected by the alignment layer and prepolymer. A solution of the LC and prepolymer, in the weight ratio of 60:40, is introduced into the cell by capillary action in the isotropic phase of the LCs. The cells are exposed to ultraviolet (UV) light of $\lambda = 350$ nm to initiate polymerization. The source of the UV light is a Xenon lamp operated at 200 W.

Fig. 1(a) shows the fabrication process for a microlens array. We used a surface relief array of hemispheres as a photomask. The surface relief structure is placed on one of the glass substrates without the PVA or N6 alignment layers. The cell with the LC + prepolymer mixture is irradiated with UV light for $\sim$ 10 min. A second exposure is performed without the relief array for 5 min to fully harden the polymer. During this process,

Manuscript received June 12, 2004; revised November 5, 2004. This work was supported by the Ministry of Science and Technology of the Korean government under the Information Display R&D Center, one of the 21st Century Frontier R&D programs.

J.-H. Kim is with Division of Electrical and Computer Engineering, Hanyang University, Seoul 133-791, Korea (e-mail: jhoon@ hanyang.ac.kr).

S. Kumar is with Department of Physics, Kent State University, Kent, OH 44242 USA (e-mail: satyen@xray.kent.edu).

Digital Object Identifier 10.1109/JLT.2004.841254

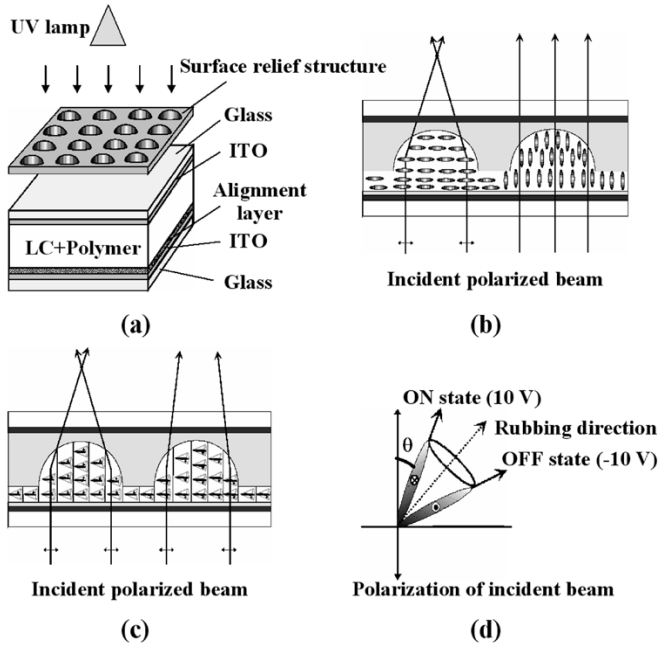

Fig. 1. Schematic diagrams of (a) fabrication setup and resultant structures with two operating states of (b) nematic and (c) FLC microlens arrays. (d) The orientation of the FLC molecules in two states in the xy plane as viewed along the direction normal to the cell. The surface relief array of hemispheres is fabricated by a UV curable polymer.

the LC molecules that remain in the polymer network after the first UV exposure are expelled from the polymerized volume. Because of the thickness-dependent absorption, a UV intensity gradient is created across the circular areas which, in turn, causes anisotropic phase separation resulting in the highest LC concentration in the middle of the shadow. Upon the completion of polymerization, an array of 3-D plano-convex structures is obtained as shown in Fig. 1(b) and (c), which act as microlenses.

The focal length f of a microlens can be calculated from

$$f = \frac{R}{n_{lc} - n_p} \tag{1}$$

where R is the radius of curvature of the lens' surface and n_{lc} and n_p are the effective LC and polymer indexes of refraction, respectively. The focal length can be changed by changing the effective value of n_{lc} with the help of an applied electric field. The value of effective n_{lc} depends on the polarization of the incident light. When the polarization is parallel to the director, the light beam sees the extraordinary refractive index $(n_{lc} = n_e = 1.762)$ of E31 in the absence of an applied field, and $f = 4.2R$. As the applied field exceeds a certain threshold value, the LC director begins to reorient along the field, and the incident beam sees a component of ordinary refractive index $(n_{lc} = n_o = 1.535)$ of E31. At the highest fields, the focal length becomes as large as 91 R. In FLCs, the directors are tilted in the smectic plane by direct coupling of the dipole moment and electric field. Fig. 1(d) depicts the molecular orientation as viewed along the cell normal.

III. Results and Discussion

A. Anisotropic Phase Separation

A complete theory of the anisotropic phase separation by UV exposure would describe the evolution of the microlens structure in terms of the special and temporal distributions of LCs, prepolymers, polymers, and all intermediate oligomers. It would also include the effects of a rubbed substrate surface on the induction of nematic ordering in otherwise isotropic LC mixtures and the polymer morphology. In our previous report [8], we developed a simple model to describe the anisotropic phase separation due to the UV intensity gradient in the direction of sample thickness (z axis) using the mean-field kinetic theory. According to the model, the LC molecules are expelled from the polymerized volume by polymerization of the prepolymer by UV light, namely, the contraction effect. Now, we consider the effect of the surface interaction between the LC/prepolymer and alignment layer on the anisotropic phase separation.

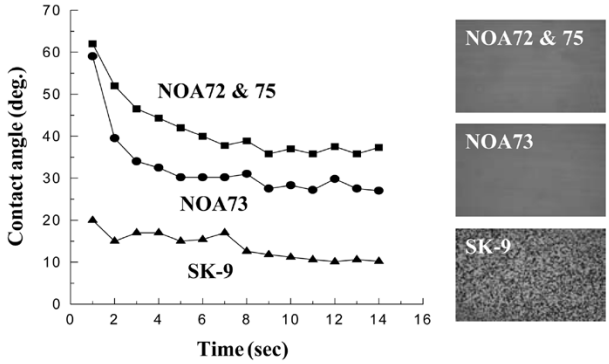

Fig. 2. Contact angles for different prepolymers on Nylon 6 as functions of time after dropping and alignment textures with nematic LC after phase separation.

Fig. 2 shows contact angles on N6 for different prepolymers as functions of time after dropping and alignment textures with nematic LC after phase separation. The contact angles were measured with a contact angle and surface tension analyzer (Phoenix 300, Surface Electro Optics Company) by taking pictures of droplets on slide glass in every second after dropping prepolymer from a microsyringe. In this experiment, we used NOA series (72, 73, and 75) from Norland, and SK 9 from Summers Laboratories. In the data, the fluctuation of contact angles according to time is within the experimental error range. The contact angles of NOA 72 and 73 saturate at more than 30° after 10 s. NOA 75 shows almost the same behavior as that of NOA 72. The contact angle of SK 9, however, saturates at 10°. This indicates that SK 9 has a stronger correlation with N6 than with the NOA series. Since the LC materials used are fully wetted on the N6 alignment layer and dewetted on the indium tin oxide (ITO) substrate, the interactions of LC and SK 9 with the surface alignment layers compete with each other and form network structures with UV exposure. With the NOA series, the LC molecules near the alignment layer respond to its anchoring potential and align parallel to the rubbing direction. Oriented LC molecules determine the microscopic structure of the polymer–LC interface, which becomes compatible with their alignment. Therefore, the presence of the alignment layer promotes the surface-induced anisotropic phase separation in the direction of sample thickness.

As a result, we successfully fabricated a phase-separated composite organic film structure that has adjacent uniform polymer and LC layers using the UV intensity gradient in the

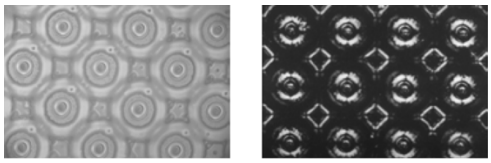

Fig. 3. Microscopic textures of a microlens array under a polarizing microscope without applying a voltage. The rubbing direction is rotated (a) 45° and (b) 0° with respect to one of the crossed polarizers. Concentric rings of different color signify changing optical thickness, and the uniform color area outside the lenses indicates cell uniformity.

z direction and surface effect as shown in Fig. 2. The theoretical model including surface potential for understanding the anisotropic phase separation is now being developed and will be published elsewhere. The use of a suitable photomask during UV exposure produces additional intensity gradients in the (xy) plane of the cell. Monomers in the high-intensity region near the UV source undergo polymerization first, and those monomers in the low-intensity region diffuse to the high-intensity region to maintain their relative concentration and join the polymerization reaction [9], [10]. The LC molecules are immiscible in and are expelled from the polymer. Therefore, we can control the anisotropic phase separation in three dimensions using a suitable photomask and alignment layer. In our experiment, we used a surface relief array of hemispheres as a photomask as shown in Fig. 1(a).

B. Nematic Microlens Array

Fig. 3 shows polarizing microscope textures of the cell after UV exposure without an applied field using nematic LC. Clearly, very regular internal structures are formed as shown in Fig. 3(a). A set of concentric circular fringes is visible in the regions that were under the surface relief hemisphere, indicating a continuous variation of the optical path length from the center to the edge. The circular rings are surrounded by relatively uniform regions. One can get a uniformly dark state outside the circular regions [Fig. 3(b)] by rotating the cell between crossed polarizers.

The focal length of these microlenses is determined by mounting the cell on a micrometer motion translation stage. It is illuminated with a collimated He–Ne laser beam (632.8 nm) from one side. Light passing through the lens is collected by an imaging lens and detected by a charge-coupled device (CCD) camera. To measure the focal length, first we focus the imaging lens on the microlens surface and then translate the lens array toward/away from the imaging lens to find the focal point. Fig. 4 shows the focusing properties of the laser beam through the lens. The polarization of the incident beam is parallel to the direction of the LC director. Fig. 4(a) shows the image of the beam focused by one microlens with no applied field. It acts as a plano-convex lens with focal length f of 1.7 mm. The light intensity profile measured at the focal point is shown in Fig. 4(b). When we apply 3 V, the beam is defocused [Fig. 4(c)] and refocused at a distance of 3.7 mm [Fig. 4(d)]. From the measured dependence of the focal length shown in Fig. 5, it is clear that f depends quadratically on the field beyond a threshold value of 1.5 V.

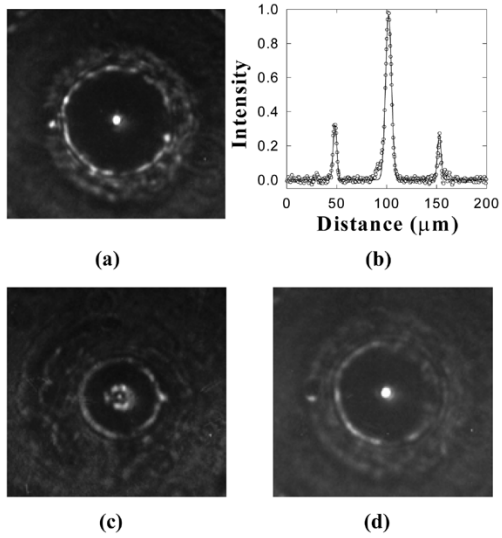

Fig. 4. Focusing properties of the laser beam through the lens. (a) Focused beam image at 1.7 mm without applying voltage. (b) Light intensity profile at the focal point. (c) Defocused beam image with 3 V at 1.7 mm. (d) Refocused beam image with 3 V at 3.7 mm.

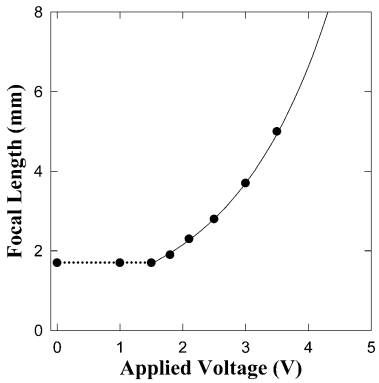

Fig. 5. Voltage dependence of the microlens' focal length. Focal length increases quadratically for fields higher than the threshold value of 1.5 V.

The switching time from the focusing to nonfocusing state and back are $\sim$ 30 and 130 ms, respectively. However, higher speeds can be achieved with FLC. The value of f is also confirmed by measuring the magnification of an object (number "15" on a reticule; 0.37×0.41 mm in size), its distance from the lens, and the position of the image using a microscope.

We note that the reproducibility and uniformity of the microlens within the array are closely related to the uniformity of the anisotropic phase separation in the cell during UV exposure. The uniform phase separation can be achieved by the uniform cell thickness, the mixing of LC and prepolymer, and UV intensity. We got uniform microlens array in the center of the cell (1 $\times$ 1 cm), where the above conditions were satisfied. The size of the microlens depends on the size of the photomask and the distance between the photomask and the cell during UV exposure. In our case, we can successfully fabricate nematic microlenses with different diameters from 100 μm to 1 mm.

To determine the geometrical shape and the value of R of these structures, a cell is opened, and the LC washed away with hexane. Fig. 6(a) and (b) shows the polymer structure under a microscope in the reflective mode and the shape profile of

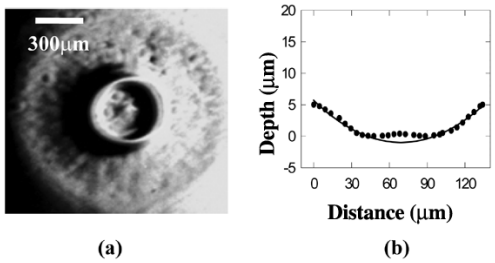

Fig. 6. (a) Microscopic structure and (b) depth profile of one of the microlenses. The line in (b) is a fit to determine the radius of curvature $R = 381 \pm 20\ \mu$m and diameter of $\sim 150\ \mu$m.

the central region using alpha-steps, respectively. The radius of curvature of the central region is determined to be $381 \pm 20\ \mu$m from the least square fit to a circle, represented by the solid line. The focal length f is calculated to be 1.6 ± 0.1 mm, in good agreement with the measured value of 1.7 mm. The curvature is also fitted with parabolic function within negligible error range. Therefore, we can conclude that a spherical aberration can be neglected. However, a chromatic aberration is unavoidable in LC-based microlenses, because the effective refractive indexes of LC (n_{lc}) are depending on wavelength and LC molecular alignment on the polymer surface.

The focused beam spot and ring structure in Fig. 4(a) comes from the crator-like central region and surrounded region, respectively. The curvature and the surrouned region of LC-polymer interface can be controlled by changing the cell thickness, the relative diffusion rates of LC and polymer, the rate of polymerization, and the shape of photomask. It is possible to fabricate microlenses of different focal lengths. With proper selection of the LC and polymer materials, it is possible to fabricate a converging $(n_{lc} > n_p)$, a diverging $(n_{lc} < n_p)$ lens, or a lens that changes from converging to diverging $(n_e < n_p < n_o)$. The microlens density and placement in the array can be controlled with the use of an appropriate photomask. The ability to individually address each lens using the well known matrix addressing schemes commonly used in LC display devices makes them very versatile.

C. Ferroelectric Microlens Array

In FLCs, the directors are tilted in the smectic plane by direct coupling of the dipole moment and electric field. Fig. 1(d) depicts the molecular orientation as viewed along the cell normal. The effective value of n_{lc} can be given as

$$n_{lc} = \frac{n_e n_o}{\sqrt{n_e \sin^2\theta + n_o \cos^2\theta}} \tag{2}$$

where θ is the angle between the polarization of the incident light and the azimuthal orientation of molecules. Fig. 7 shows the calculated focal length as a function of θ. We found that the focal length diverges at $\theta = 62^\circ$. Since the tilt angle of the FLC is measured as 20° at room temperature, the best switching characteristics of the lens are obtained between 22° and 62° as shown in Fig. 1(d). In our experiment, however, the focal length diverges at $\theta = 65^\circ$ because the LC medium is dispersive.

Fig. 8 shows a polarizing microscope picture of the FLC microlenses with different diameters (a) 355 and (b) 225 μm after UV exposure without an applied field. The diameters are

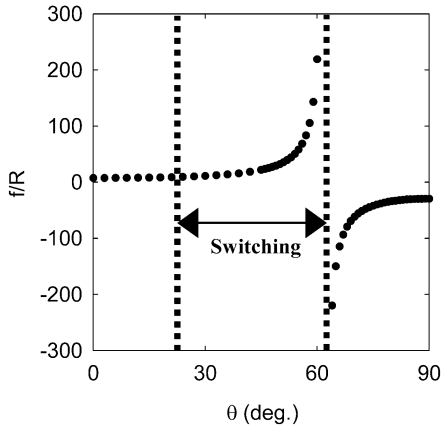

Fig. 7. Calculated focal length as a function of smectic tilt angle θ using (1) and (2) (see text). The tips of the arrows indicate the two stable operating states shown in Fig. 1(d).

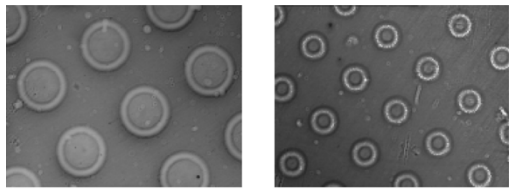

Fig. 8. Microscopic picture of two microlens arrays, with (a) 355 μm and (b) 225 μm in lens diameter, as viewed through a polarizing microscope without any applied voltage.

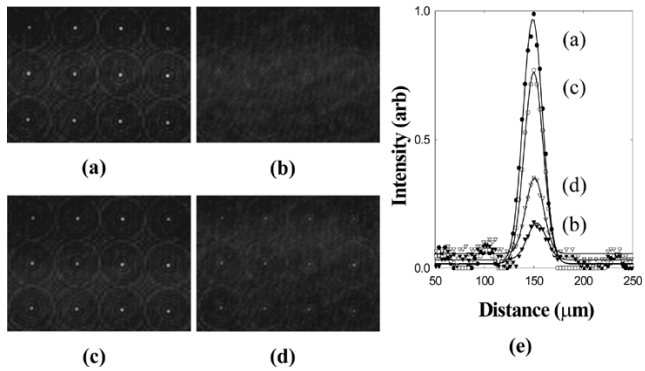

Fig. 9. Focusing characteristics of microlens for a laser beam passing through the lens of 355 μm in diameter. (a) and (b) are beam images at 11 mm with ± 10 V, respectively. Panels (c) and (d) show the images of the beam with applied voltages of ± 10 to 0 V, respectively. (e) Profiles of the transmitted light beam in (a) and (d).

controlled by using different diameter hemispheres in the surface relief structures. Clearly, very regular internal structures are formed in the shadow of the surface-relief hemispheres indicating a continuous variation of the optical path length from their center to edge. The circular rings are surrounded by relatively uniform regions. One can get a uniformly dark state outside the circular regions by rotating the cell between crossed polarizers. We note that the size of the FLC microlens is dependent on the diameter of hemisphere, UV intensity, and the distance between the photomask and the LC cell.

Fig. 9 shows the focusing properties of the laser beam through a lens with a diameter of 335 μm. Fig. 9(a) and (b) shows the images of the beam with a potential difference of 10 and -10 V,

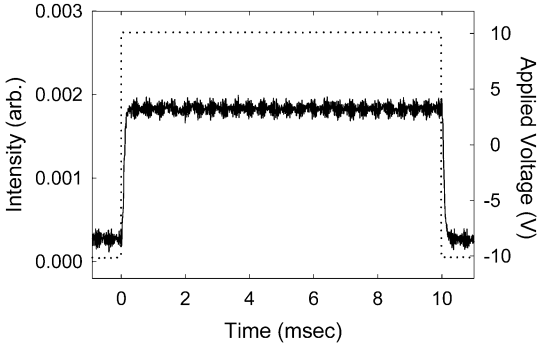

Fig. 10. Transmission versus time curve for an FLC microlens. The ON and OFF times are 150 and 88 μs, respectively.

respectively, applied across the lens. With 10 V, the focal length is found to be 11 and 7.5 mm for the two lenses with diameter of 355 and 225 μm, respectively. In this case, the director of the FLC is oriented at 25°, and the incident beam sees an effective refractive index (n_{lc}) of 1.628. Therefore, the beam is focused. When we apply -10 V, the director of the LC is reoriented at 65°. At this angle, the focal length diverges as shown in Fig. 7. Therefore, the beam is defocused. Fig. 9(c) and (d) shows the images of the beam when the applied voltage is changed from ± 10 to 0 V. The intensity profiles for these situations are shown in Fig. 9(e). The intensities are slightly different in (c) and (d) with respect to (a) and (b), respectively, demonstrating the memory effect of these FLC microlenses. The extinction ratio of the two beams are approximately 1:2. The slight changes in the intensities are due to the remaining polymer in the FLC layers. If we reduce the polymer content, it is possible to obtain high-extinction and bistable microlenses. It should be noted that the bistability also depends on the thickness of the cell. With a thicker cell $(> 5\mu\text{m})$, we found that the beam intensity varied continuously.

In Fig. 10, we present the switching characteristics of a focused laser beam. The times to turn the lenses ON and OFF are 150 and 88 μs, respectively. We measured the switching time using an oscilloscope by measuring the time of intensity variation between 10% and 90% of the maximum intensity. We note that the switching time of nematic microlenses was measured to be of the order of 100 ms. Evidently, and as expected, the switching times of FLC microlenses are about 1000 times faster than the NLC microlenses. We believe that these devices will find applications in optical communications technology in the near future.

IV. Conclusion

In this paper, a new method for the fabrication of an electrically controllable two-dimensional microlens array was proposed and demonstrated. The lens array is fabricated by an anisotropic phase separation from a composite of a UV curable polymer and a LC. The focal length varies with the applied voltage as well as the concentration of the LCs and the sample thickness. Specifically, two-dimensional FLC microlens arrays have very fast switching times, ones that are three orders of magnitude faster than for similar devices built using nematic LCs. Furthermore, the FLCs exhibit a memory effect. Because of the internal structure, they possess the capability of withstanding high mechanical stress and are likely to possess high efficiency and transmission. Furthermore, they can be prepared on flexible, thin, and low-weight substrates. They should prove to be valuable in focused beam steering, active-fiber star couplers for high-density optical communications, parallel interconnects for neural networks, and optical limiters, as well as other military applications.

References

[1] T. Nose and S. Sato, "A liquid crystal microlens obtained with a nonuniform electric field," *Liq. Cryst.*, vol. 2, p. 1425, 1989.
[2] T. Nose, S. Masuda, S. Sato, J. Li, L. Chien, and P. Bos, "Effects of low polymer content in a liquid-crystal microlens," *Opt. Lett.*, vol. 22, p. 351, 1997.
[3] M. N. F. Borrelli and O. L. Morse, "Microlens arrays produced by a photolytic technique," *Appl. Opt.*, vol. 27, p. 476, 1988.
[4] M. Wang and H. Su, "Multilevel diffractive microlens fabrication by one- step laser-assisted chemical etching upon high-energy-beam sensitive glass," *Opt. Lett.*, vol. 23, p. 876, 1998.
[5] M. Fritze, M. Stern, and P. Wyatt, "Laser-fabricated glass microlens array," *Opt. Lett.*, vol. 23, p. 141, 1998.
[6] K. Rastani, C. Lin, and J. S. Patel, "Active-fiber star coupler that uses arrays of microlenses and liquid-crystal modulators," *Appl. Opt.*, vol. 31, p. 3046, 1992.
[7] Vorflusev and S. Kumar, "Phase-separated composite films for liquid crystal displays," *Science*, vol. 283, p. 1903, 1999.
[8] T. Qian, J.-H. Kim, S. Kumar, and P. L. Taylor, "Phase separated composite films: Experiment and theory," *Phys. Rev. E, Stat. Phys. Plasmas Fluids Relat. Interdiscip. Top.*, vol. 61, p. 4007, 2000.
[9] Krongauz, E. Schmelzer, and R. Yohannan, "Kinetics of anisotropic photopolymerization in polymer matrix," *Polymer*, vol. 32, p. 1654, 1991.
[10] X. Wang, Y. Yu, and P. L. Taylor, "Kinetic theory of phase separation induced by nonuniform photopolymerization," *J. Appl. Phys.*, vol. 80, p. 3285, 1996.

Jae-Hoon Kim received the B.S. degree from Sogang University, Seoul, Korea, in 1987, the M.S. degree from the University of Oregon, Eugene, and the Ph.D. degree from Sogang University, in 1996, all in physics.

He formerly worked at the Liquid Crystal Institute, Kent State University, Kent, OH, as a Research Associate from 1996 to 1999. From 1999 to 2000, he was with Samsung Electronics, Giheung, Korea, where he was involved in the development of patterned vertical alignment liquid-crystal displays. In 2000, he joined the Department of Physics of Hallym University, Chuncheon, Korea, as an Assistant Professor. Since March 2004, he has been an Associate Professor in the Division of Electrical and Computer Engineering, Hanyang University, Seoul, Korea. His main research interests include display and photonic devices using liquid crystals.

Satyendra Kumar received the B.Sc. and M.Sc. (Hons.) degrees from Panjab University, Panjab, India, in 1974, the M.S. degree in physics from the University of Nebraska, Lincoln, in 1975, and the Ph.D. degree in high-resolutions X-ray studies of liquid crystals from the University of Illinois, Urbana-Champaign, in 1981.

He then joined the Massachusetts Institute of Technology, Cambridge, as a Postdoctoral Research Associate and performed research on quasi-elastic light scattering and X-ray diffraction studies of structure and critical phenomena. In 1984, he joined Tektronix, Inc., Beaverton, OR, to develop an electron-beam-addressed light valve for video projection displays. In 1987, he joined the Department of Physics and Liquid Crystal Institute, Kent State University, Kent, OH, where he is now Professor of the physics and chemical physics interdisciplinary program.